

# We are IntechOpen, the world's leading publisher of Open Access books Built by scientists, for scientists

6,900

Open access books available

185,000

International authors and editors

200M

Downloads

Our authors are among the

154

Countries delivered to

TOP 1%

most cited scientists

12.2%

Contributors from top 500 universities



WEB OF SCIENCE™

Selection of our books indexed in the Book Citation Index  
in Web of Science™ Core Collection (BKCI)

Interested in publishing with us?  
Contact [book.department@intechopen.com](mailto:book.department@intechopen.com)

Numbers displayed above are based on latest data collected.  
For more information visit [www.intechopen.com](http://www.intechopen.com)



---

# Rheology of Highly Filled Polymers

---

Christian Kukla, Ivica Duretek,  
Joamin Gonzalez-Gutierrez and Clemens Holzer

Additional information is available at the end of the chapter

<http://dx.doi.org/10.5772/intechopen.75656>

---

## Abstract

In many applications and/or manufacturing processes, highly filled polymers are necessary. One of these fields is powder metallurgy, where polymers or polymer mixtures are used to enable the shaping process within the production of the parts. Metal and also ceramic powders are mixed with different polymeric substances with a powder content of more than 50 vol%. Within the production, this mixture, called feedstock, has to flow into the final shape. Thus, for a proper understanding of the production processes, fundamental knowledge on the flow behavior of the feedstocks is required. For the rheology of polymers, several techniques together with the proper equipment are available. In the case of high viscosities, rotational and high-pressure capillary rheometers (HPCRs) are used. To gain reliable data, a proper measurement procedure is essential, which means that the operator has to have a deeper physical understanding of the material and the effects arising during the measurements. Therefore, this chapter gives an insight into rotational and high-pressure capillary rheometry with special emphasis on the behavior of polymers highly filled with stiff particles. Based thereon important remarks on the measurement equipment, procedure and evaluation of the measured data are provided.

**Keywords:** rheology, polymer, highly filled, feedstock, plate-plate rheometer, high-pressure capillary rheometer, yield stress, powder loading, Bagley correction

---

## 1. Introduction

The addition of inorganic or organic fillers into polymeric materials is an effective way to attain certain desirable properties for different applications [1]. The rheological behavior is dependent on the amount of fillers in the liquid polymer. Other factors influencing the viscosity of the highly filled polymers are the particle size and shape, the particle size distribution,

the nature of the filler and the polymer matrix, as well as the use of coupling agents or compatibilizers. A detailed description of these influencing factors is given in [1].

For very dilute systems, the fillers are sufficiently apart that the interaction between them is negligible, and their rheological behavior is drastically changed when the concentration increases beyond 15 vol%, approaching a solid-like behavior [2]. However, the critical volume fraction, at which the solid-like behavior is observed, is a function of the particle shape and size distribution [1]. In this chapter, we discuss the flow behavior of filled polymers with a particle concentration well above 15 vol%, where the interparticle interaction cannot be ignored; these materials are referred to as highly filled polymers. Highly filled polymers have found applications in many industries including the adhesive, dental, battery, ceramic, metallurgy, electronics packaging, and solid propellant industries; therefore, understanding their flow behavior is crucial for many industrial applications [1].

In the literature, a wide variety of models to describe the dependence of the viscosity of mainly the volume concentration of the filler  $\phi_p$  is available [3–12]. Other parameters like shape factors or interactions between the particles are also taken into account [1, 13]. Einstein was the first to address the suspension behavior in the dilute limit theoretically ([4], corrected 1911 [5]). Later on, further models have been developed. Regarding the concentration of the filler as the main parameter, these models can be structured into two groups [13]:

- Exponential models (Mooney [10] type) and
- Power-law models (Krieger [9] type)

In addition to [1, 13], we show in this chapter some models with a flow behavior integrating a yield strength.

Particular applications of highly filled polymers in the ceramic and metallurgy industries are ceramic injection molding (CIM), metal injection molding (MIM), and fused filament fabrication (FFF) [14, 15]. FFF is a special variant of material extrusion (ME) additive manufacturing (AM). In CIM, MIM, and FFF, a polymeric blend is used as a carrier or binder material for stiff powders during the fabrication of ceramic and metallic parts with complex geometry. Since the final part obtained at the end of these processes must be metal or ceramic, the filler content should be larger or equal to 50 vol% [15]. Measuring the rheological behavior of these materials is crucial to ensure that the correct processing conditions (e.g., for injection molding or extrusion) are used. Thus, it is one of the main motivations and backgrounds for preparing this chapter.

In this chapter, the methods used to measure the rheological properties of highly filled polymers with stiff fillers together with special issues or features of the rheological behavior of highly filled polymers are discussed in Section 2, and models used to describe the viscosity of highly filled polymers are explained in Section 3.

## 2. Measurement methods

Rheometers can be divided into two groups. In the first group, a material is dragged along a moving wall (like rotational rheometers), while in the second group, the sample is forced

through a channel, cylindrical pipe, or slit by means of pressure (like high-pressure capillary rheometers (HPCRs)) [2]. In this section, the specific details of performing rheometry on highly filled polymers with both types of rheometers are presented. It is important to remember that in order to have a complete rheological characterization of highly filled polymers both rheometers are needed to cover the range of shear rates that could occur during different processing operations [16].

## 2.1. Rotational rheometer

A rotational rheometer consists of a rotating or oscillating geometry and a fixed geometry; between these two geometries, the sample is sheared by a known torque when using a controlled shear stress (CSS) rheometer or a known deformation rate when using a controlled strain rate (CSR) rheometer. Several measuring geometries are available for rotational rheometers of polymeric materials; the most common examples are concentric cylinders (Couette or Searle Type), cone plates, and parallel plates (or disks) [2]. For highly filled polymers, parallel plates are the preferred measuring geometry (**Figure 1**). The main reason for using parallel plates is that the measuring gap can be adjusted. The high content of solid rigid particles in highly filled polymers could prevent reaching gaps smaller than 0.5 mm, which are required when using truncated cone-plate geometries and certain types of concentric cylinders. It is recommended that the measuring gap be at least 10 times larger but not larger than 50 times than the largest particle inside a suspension [2].

In order to satisfactorily measure rheological data in a rotational rheometer, two conditions need to be satisfied:

- i. the sample must adhere to the plate surface and
- ii. the flow must be laminar.

For highly filled polymers, adhesion to the plate surface can be complicated since the filler particles may be in direct contact with the plate surface and thus reduce the friction. Over time also particle migration or sedimentation might contribute to the formation of a low-viscosity depleted layer between the plate surface and the bulk of the fluid. Both conditions could lead to slip effects. In order to prevent slip from happening, it is recommended to use serrated plates (instead of smooth plates), as shown in **Figure 2**. The serrated plates provide enough grip between the sample and the measuring plates; thus, the sample is

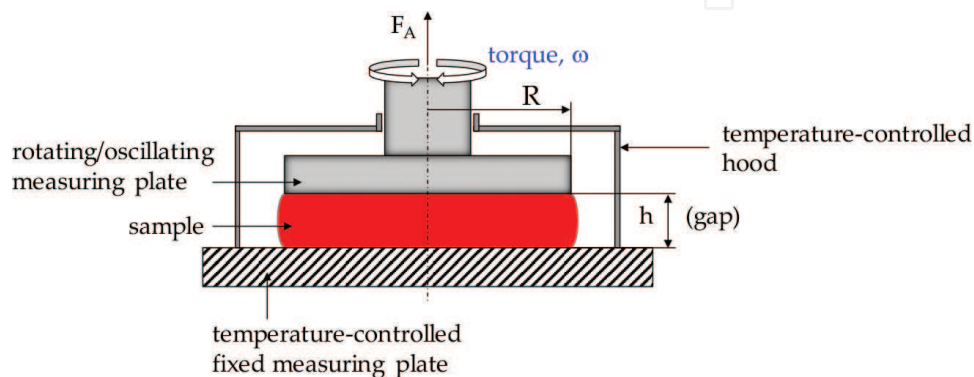


**Figure 1.** Schematic drawing of the parallel plate rheometer.

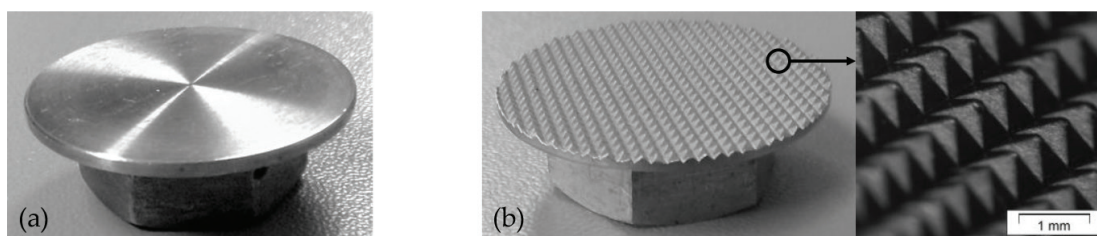


**Figure 2.** Measuring plate geometries: smooth (a) and serrated (b).

homogeneously sheared throughout its bulk, satisfactorily preventing slip. Using deep channels or smaller features on the plate is not sufficient to prevent slip during rotational rheometry measurements as it has been shown elsewhere [16].

For highly filled polymers, it is recommended to use a measuring gap between 0.5 and 1.5 mm and serrated plates with a diameter between 20 and 25 mm. The sample should be prepared by pressing the highly filled polymeric pellets into disks of slightly larger dimensions than the selected measuring plate and the desired gap, in order to ensure reaching the selected gap without air gaps in the highly viscous sample. Once the measuring temperature is selected and the measuring chamber has reached the set temperature, the sample can be introduced. When it has reached the measuring temperature, the movable plate is slowly brought to the measuring gap. It is important to remove the excess material coming out from between the measuring plates and that the normal force is zero before starting the measurement in order to prevent artificially increasing the measured viscosities. In a previous investigation, it was observed that a tenfold increased normal force leads to a viscosity increase of one order of magnitude [16].

Viscosity measurements of highly filled polymers are usually performed in constant rotational mode and not in the oscillatory mode because the Cox-Merz rule [17] is not valid for highly filled polymers (see also Section 2.6). The shear rate range for highly filled polymers is also quite narrow ( $10^{-4}$  to  $10^{-1} \text{ s}^{-1}$ ). The large amount of fillers leads to a yield stress near the zero shear stress limit, and therefore, a high viscosity value is observed at low shear rates [18]. Once the rotating plate starts to move, the filler particles start to orient in the direction of flow and therefore a clear shear thinning behavior is observed for most highly filled polymers. Continuously shearing the sample eventually leads to melt fracture and sample expulsions, which lead to an abrupt and irreversible drop in the viscosity; therefore, only the viscosity measurements before melt fracture should be considered [2]. Sample expulsion is very common and can occur already at shear rates of  $10^{-1} \text{ s}^{-1}$ , but this depends on the filler content and the type of polymer.

When measuring highly filled polymers, preshear should be applied. This is especially important for thixotropic materials and those materials that show a yield stress. This can be used to set the initial state of the sample and increase the repeatability of rheological measurements of highly filled polymers [2].

Finally, care should also be taken when selecting the time of the experiment, since prolonged exposure to temperatures above the melt temperature of the suspending polymers could lead to chemical changes in the sample [2]. Furthermore, it is always recommended to perform rotational rheometry measurements in an oxygen-free atmosphere and not to use high shear rates.



## 2.2. High-pressure capillary rheometer

The high-pressure capillary rheometer (HPCR) allows the routine analysis of the flow and viscosity of polymer melts at shear rates from 10 to  $10^6 \text{ s}^{-1}$ . The realizable shear rate range depends on the viscosity of the tested material, the measurement temperature, and the used die geometry (e.g., round die or slit die).

The HPCR comprises a temperature-controlled test barrel and an exchangeable die at its end. The geometry of the die is variable. The melt inside the test barrel is pressed through the round or slit die by means of a test piston. When all test parameters are defined and the system reaches the test temperature, the test barrel can be filled with polymer granulate. In order to fill it bubble free, the material should be filled in portions. After each portion, the material should be pressed manually with a tamper or with the test piston. The measurement is ready to begin when the test barrel is full. Then, the preheat time (or melting time) starts. At the end of the preheat time, the test starts automatically by the movement of the piston with the first preselected feed rate. The melt pressure is measured by using mounted pressure transducers before the round die or along the slit length of the slit die (**Figure 3**). As soon as the pressure varies exactly within the tolerance limit, the speed of the piston is recorded. Therefrom, the apparent viscosity data are calculated immediately. At the same time, the piston speed is increased to the next value. In this way, the whole speed program is run step by step.

In the following section, the two types of dies used for HPCR are presented together with a discussion of important points one should be aware of when measuring viscosities with them.

### 2.2.1. Round die

High-pressure capillary rheometers with round dies (**Figure 3**, left) are widely used in polymer melt rheometry. Round dies exist in different lengths with the same diameter (e.g.,

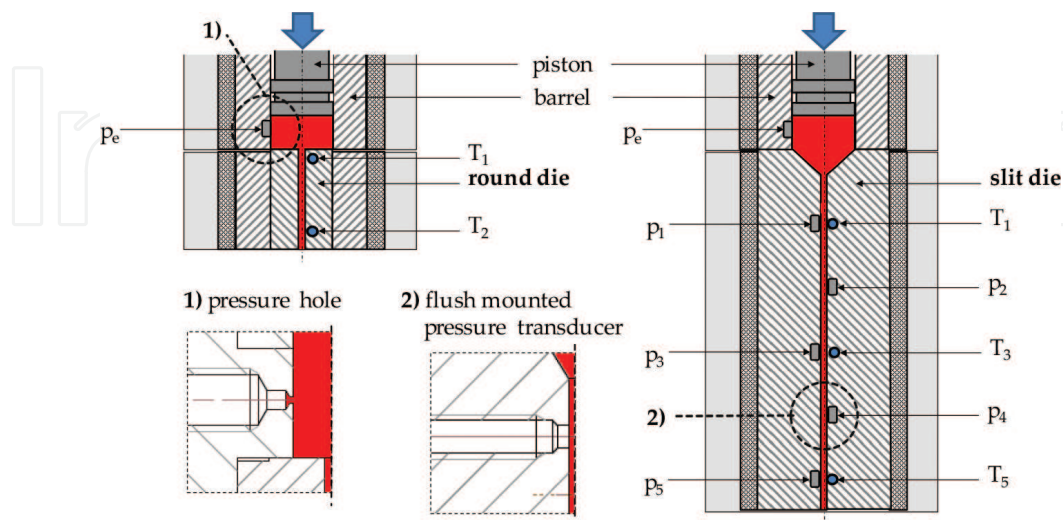


**Figure 3.** Schematic drawing of the high-pressure capillary rheometer with the round and slit die; p—Pressure transducers and T—Thermocouple (wall temperature).

$L/D = 10, 20$ , and  $30$ ). The entrance angle of a round die is  $180^\circ$ . To measure the temperature near the die wall, thin thermocouples can be attached to the die as shown in **Figure 3**.

From geometrical data, the speed of the piston, and the related pressure drop, the so-called apparent viscosity is calculated [19]. In order to obtain the correct viscosity of polymeric materials, two corrections are commonly applied to round dies data: the Bagley correction [20] and the Weissenberg-Rabinowitsch correction [21]. The Bagley correction takes care of the nonideality arising from viscoelastic effects at the entrance of the die. During the melt flow in the die inlet, outlet pressure losses develop. For the correction of these inlet and outlet pressure losses, the Bagley correction can be used. Therefore, several measurements with capillaries with the same diameter but with different lengths have to be done.

The plotted measured pressures ( $p_{\text{meas}}$ ) in front of the die versus  $L/D$  ratio in general can be described by a linear function for each individual shear rate. The extrapolation of these straight lines to the  $L/D$  ratio = 0 provides the pressure correction value  $p_{\text{en}}$  mentioned in Eq. (1) [21].

$$\tau_O = \frac{(p_{\text{meas}} - p_{\text{en}}) \cdot R}{2 \cdot L} \quad (1)$$

where  $\tau_O$  is true shear stress,  $p_{\text{en}}$  is entrance pressure loss, and  $R$  is die radius.

The apparent shear rate for round die  $\dot{\gamma}_{\text{app},O}$  is calculated by using Eq. (2) [19].

$$\dot{\gamma}_{\text{app},O} = \frac{4 \cdot \dot{V}}{\pi \cdot R^3} \quad (2)$$

with  $\dot{V}$  as the volumetric flow rate.

The Weissenberg-Rabinowitsch correction for the round die (Eq. (3)) considers the fact that the shear rate mentioned in Eq. (2) is only valid for Newtonian fluids and provides the true shear rate at the capillary wall for them [22].

$$\dot{\gamma}_O = \frac{\dot{\gamma}_{\text{app},O}}{4} \left( 3 + \frac{d \log \dot{\gamma}_{\text{app},O}}{d \log \tau_O} \right) \quad (3)$$

Finally, the true viscosity is calculated from Eq. (4).

$$\eta = \frac{\tau_O}{\dot{\gamma}_O} \quad (4)$$

### 2.2.2. Slit die

In the slit die, the pressure gradient, which is used to calculate the viscosity, is measured by using a series of pressure transducers along the length of the slit. **Figure 3**, right, gives a schematic drawing of the HPCR with slit die. The pressure profile along the slit die is measured by melt pressure transducers  $p_1$  to  $p_5$ . The pressure transducer  $p_e$  gives the pressure at the die entrance. The temperature at the die wall is recorded by using thermocouples, which are fixed very near to the inner wall of the slit. The slit die has the rectangular channel of width ( $B$ ) and height ( $H$ ).

The pressure drop  $\Delta p$  can be determined by taking the difference of two pressures measured along the flow length and the corresponding distance  $\Delta L$  between the pressure transducers. Thus, no Bagley correction is necessary when the pressure drop is measured along the slit. However, a so-called shape factor  $F_p$  [23] in Eq. (7) might be employed to account for the influence of the width in the rectangular flow channel [19]. The true shear stress  $\tau_w$  can be calculated from the measured pressures along the slit length and geometrical parameters of slit die, by using Eq. (5) [24].

$$\tau_w = \frac{\Delta p \cdot H}{2 \cdot \Delta L} \quad (5)$$

Eq. (5) is applicable when the ratio  $B/H$  is greater than 40; in other cases,  $\tau_w$  is given by [19]

$$\tau_w = \frac{\Delta p \cdot (B \cdot H)}{2 \cdot \Delta L \cdot (B + H)} \quad (6)$$

The apparent shear rate  $\dot{\gamma}_{app,w}$  is given by Eq. (7) [23].

$$\dot{\gamma}_{app,w} = \frac{6 \cdot \frac{\dot{V}}{F_p}}{B \cdot H^2} \quad (7)$$

The Weissenberg-Rabinowitsch correction (Eq. (8)) adjusts the shear rate at the wall for the non-Newtonian liquids. The true shear rate at the wall for a slit die ( $\dot{\gamma}_w$ ) is calculated by [22]:

$$\dot{\gamma}_w = \frac{\dot{\gamma}_{app,w}}{3} \left( 2 + \frac{d \log \dot{\gamma}_{app,w}}{d \log \tau_w} \right) \quad (8)$$

Finally, the true shear viscosity is calculated by using Eq. (9).

$$\eta = \frac{\tau_w}{\dot{\gamma}_w} \quad (9)$$

**Figure 4** summarizes the calculation of the viscosity from measurements using round or slit dies in the form of a flowchart.

### 2.2.3. Remarks on Bagley correction

In general, the pressure curves show straight lines with a certain negligible nonlinearity in **Figure 5**, left. Highly filled polymers like some MIM feedstocks can exhibit nonlinear Bagley curves that give negative entrance pressure losses when linearized, which has no physical meaning.

**Figure 5**, right, shows the results of the Bagley extrapolation on an MIM feedstock. The linear approximation of the measured values results in negative entrance pressure losses. The reasons for this can be the pressure dependence of the viscosity [25] and errors in the pressure measurement by using of pressure holes, especially in the low pressure range. A pressure hole is generally used when using round dies (insert 1 in **Figure 3**) since it is not possible to



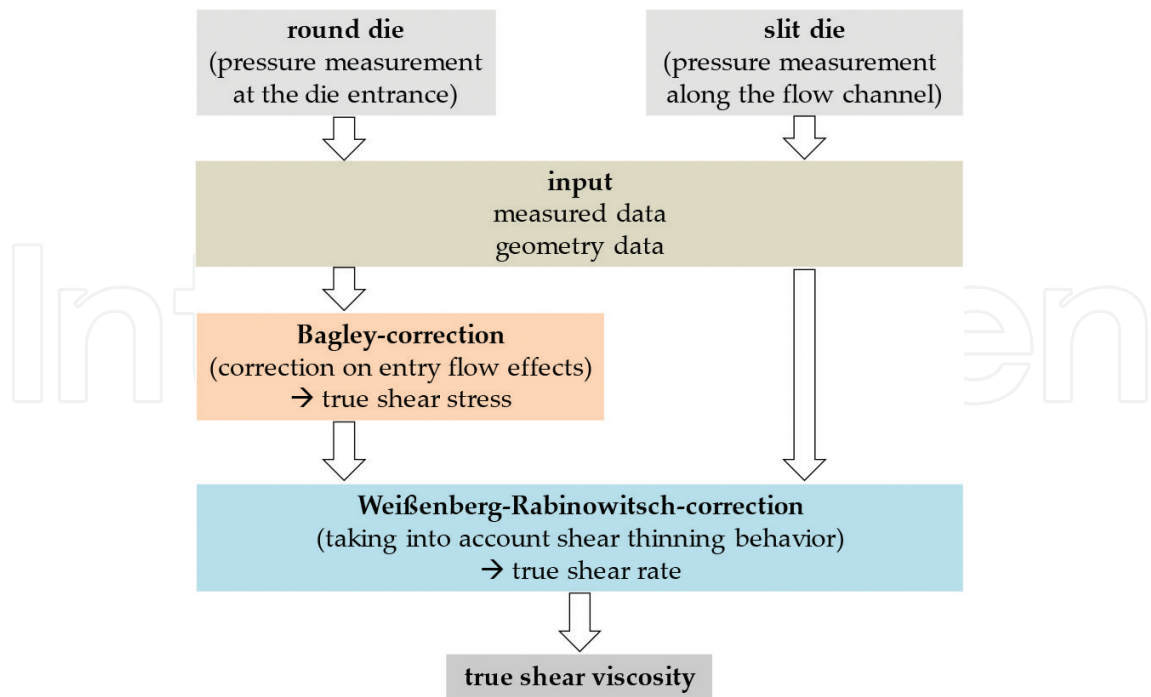


Figure 4. Flowchart of the process used to calculate the true viscosity.

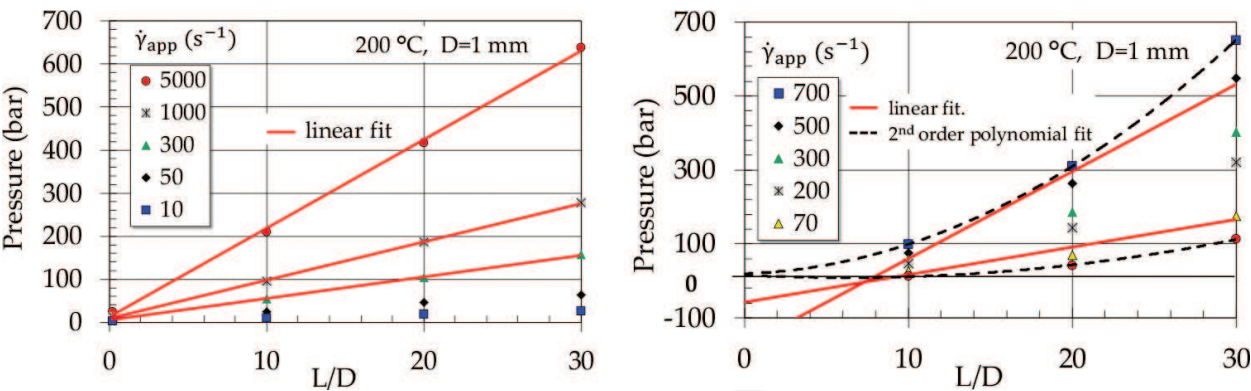
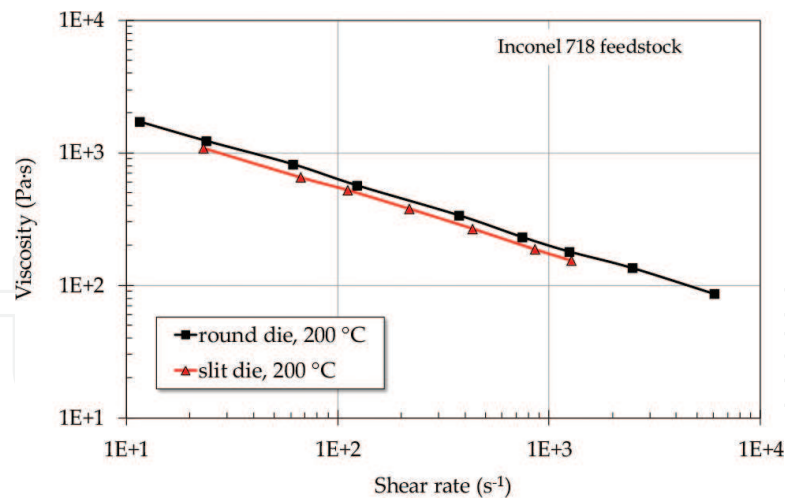


Figure 5. Bagley diagram. IN718 feedstock (left) and 316LS feedstock [28] (right).

mount a pressure transducer flush to the wall of a round die as in a slit die (insert 2 in **Figure 3**). The occurrence of wall slip and different particle distributions can also lead to nonlinear Bagley plots. Nyborg [26] and Bilovol [27] also reported negative entrance pressure losses from measurements on MIM feedstocks.

#### 2.2.4. ‘Pressure hole effect’

The comparison of the viscosities of an MIM feedstock measured with round and slit dies at a temperature of 200°C is shown in **Figure 6**. The viscosity measured with the round die ( $D = 1 \text{ mm}$ ) is about 16% higher than that of the slit die ( $H = 1 \text{ mm}$ ). The cause of this difference may be related to anisotropic pressure propagation in the pressure measurement when



**Figure 6.** Comparison of the viscosity measured with round and slit die for IN718 feedstock; measurement at the high-pressure capillary rheometer.

using a pressure hole (insert 1 in **Figure 3**). We are dealing with highly filled polymers with more than 50 vol% of powder, and a network of powder grains is no good means for pressure propagation. This refers to the potential source of error termed “pressure hole effect” [29–31].

#### 2.2.5. Pressure fluctuations

Pressure is one of the most important parameters in viscosity calculation. In rheological measurements, the pressure is determined in such a way that for each shear rate, the disturbances in the pressure values must be less than 1%. Usually, these pressure fluctuations are higher in highly filled compounds. They are dependent on the filler content and particle size.

The pressure profile measured with the slit die ( $H = 1$  mm) on PE compound with flame retardant  $\text{Al}(\text{OH})_3$  shows considerable pressure fluctuations up to  $\pm 50$  bar ( $\pm 14\%$ ) and more (**Figure 7**, left). The melt strand coming out of the slit die showed a cyclic change between smooth and wrinkled (**Figure 7**, left, inserted photo) and the measured pressure is clearly unsteady (**Figure 7**, left, inserted diagram). This can be attributed to the stick-slip effect. The pressure profile measured with the slit die on a titanium feedstock also shows considerable pressure fluctuations up to  $\pm 20$  bar and more (**Figure 7**, right).

#### 2.2.6. Influence of preshearing history on viscosity and homogeneity

Earlier rheological investigations [33–35] showed that the shearing in the plasticizing cylinder of the injection molding machine has a significant influence on the flow behavior of MIM feedstocks.

**Figure 8** shows the viscosities of 316LA MIM feedstock measured with the same slit die on the high-pressure capillary rheometer and on the injection molding machine rheometer at three temperatures. The slit die of the capillary rheometer was mounted on the injection molding machine (IMM) with the appropriate adapter [35]. As expected, both measurements give the

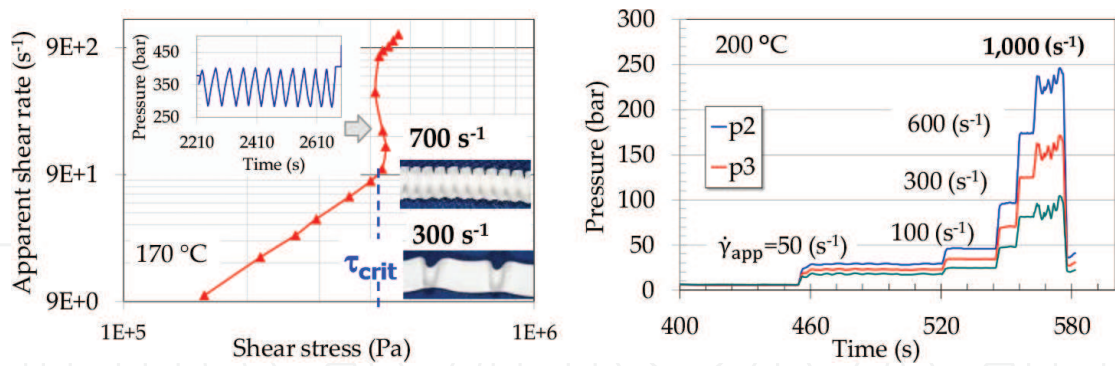


Figure 7. Stick and slip effect. PE compound with flame retardant Al(OH)<sub>3</sub> [32] (left) and Ti feedstock (right).

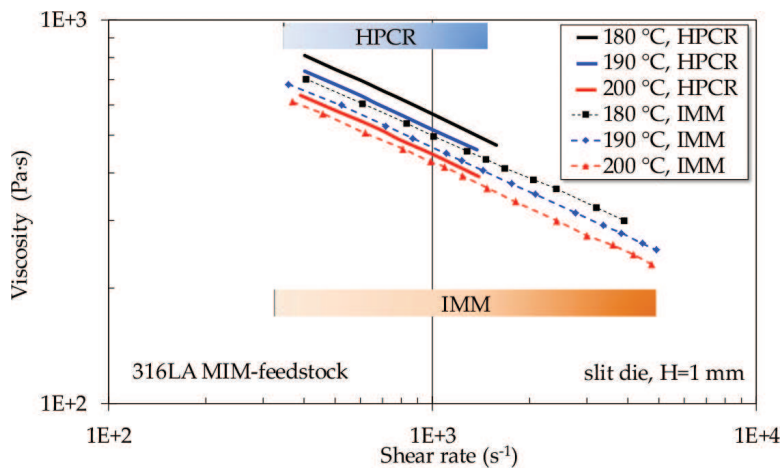


Figure 8. Comparison of viscosity measurements on high-pressure capillary rheometer (HPCR) and injection molding machine (IMM) [35].

similar slope of viscosity curves but at different levels. The viscosities measured at the injection molding machine are lower than those at HPCR. The most likely reason is preshearing of the melt by the screw during plasticization. This leads to better homogenization of the feedstock. Furthermore, the temperature distribution within the melt in the plasticizing cylinder of the IMM could also have an influence.

### 2.3. Yield stress

In contrast to unfilled thermoplastics for highly filled polymers at very low shear rates, no Newtonian plateau is observed but instead the viscosity increases strongly. This indicates the possible presence of the limiting shear stress also known as yield stress or yield point. The yield stress is classically defined as the minimum shear stress that must be applied to the material to initiate flow. In addition, yield stress is generally denoted as the transition stress at which a material behaves either as elastic solid-like or viscous liquid-like. This transition usually occurs within a range of stresses, in which the material exhibits viscoelastic behavior [36, 37]. Moreover yield stress can be defined as the force per unit area necessary to overcome interparticle interactions and its magnitude is determined by the overall strength of

the interparticle network. When the stress exceeds the yield stress, the fluid will flow like a viscous fluid with a finite viscosity.

The most common way for determining the yield stress is from a flow curve measured on a rheometer. It involves the extrapolation of the flow curve to zero shear rate using mathematical models such as Bingham, Herschel-Bulkley, Cross-Herschel-Bulkley, or CARPOW.

When using models based on measurements with the HPCR only, accuracy could be not satisfying, because the HPCR gives data only at higher shear rates, which have to be extrapolated to zero.

A better method for the yield point determination is by the rotational rheometer, preferably in the controlled shear stress (CSS) mode. Here, by plotting deformation  $\gamma$  versus shear stress  $\tau$  in a double logarithmic scale, two regions with different slopes exist (**Figure 9**, right). The first one (lower slope) is the elastic deformation region, while the second one (steeper slope) is the viscous flow region. The yield stress can be detected as the transition point in the slope of the two power law regressions [38].

CSS is more sensitive and provides more accurate results of yield stress than CSR. Better results are obtained by a combination of CSS measurements (low shear rates) and high-pressure capillary rheometer measurements (high shear rates).

It is evident that the choice of the method or model yields different values of yield stress. However, the accuracy depends on the sensitivity of the equipment and the skills of the operator. The previous investigations [39] show there is no single best method to measure yield stress of highly filled polymers, such as MIM feedstock.

## 2.4. Powder loading

A second important point for highly filled polymers is that the viscosity is a function of the characteristics of the powder and of the volume powder content  $\phi_p$ . It has been observed that the viscosity of concentrated suspensions, including MIM and CIM feedstocks, increases rapidly and nonlinearly as the solid content increases [8].

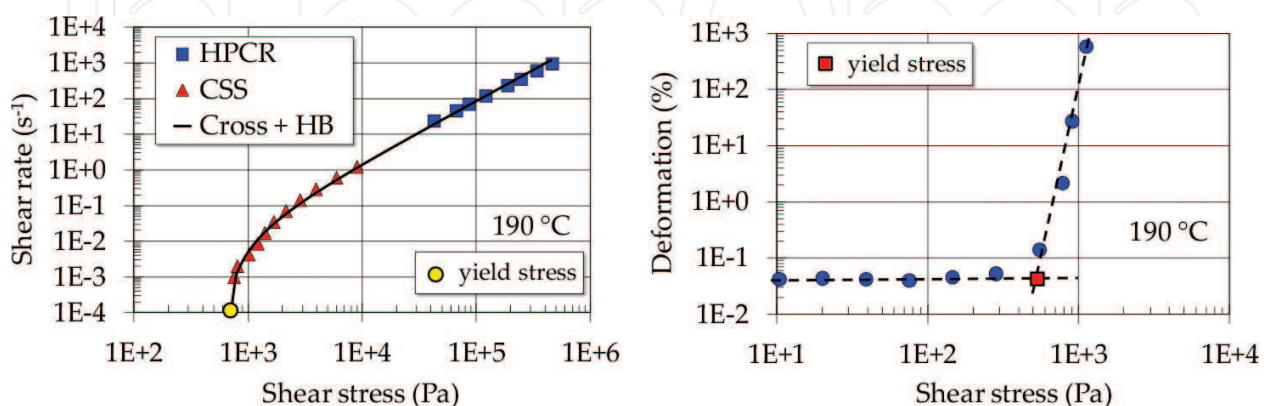


**Figure 9.** Flow curve measured with rotational (CSS) and high-pressure capillary rheometer (HPCR) for 316 L feedstock: fitting the experimental curves using Cross-Herschel-Bulkley model (left) and determination of the yield stress with rotational rheometer, CSS (right) [40].

**Figure 10** shows the comparison of the measured to the calculated increase in viscosity by increasing  $\phi_p$  of the feedstock at shear rate of  $100 \text{ s}^{-1}$ . Here the relative viscosity  $\eta_r$  is used, which is the ratio of the viscosity of the feedstock with a certain powder loading to the viscosity of the polymeric binder system at a given shear rate and temperature. For lower powder loadings, the Frankel-Acrivos model [6] provides a better fit to the measured data; for higher powder loadings, the Krieger-Dougherty model [9] is better. It has to be emphasized that the fit is dependent also on the shear rate at which the data were measured and other models available in the literature might fit better [12].

Most of the models in the literature and also the ones used in **Figure 10** are shifting the viscosity curve along the y-axis in a double logarithmic viscosity-shear rate diagram as the powder content increases (**Figure 11**, green arrow). This does not describe the behavior of feedstocks in a proper way. One main point is the shear rate at which the transition from Newtonian to shear thinning behavior takes place. This shear rate is a function of the powder loading  $\phi_p$  and cannot be described by the models mentioned before [12]. Geisbüsch [42] used a model which is based on the fact that the binder is sheared more when more powder is in the feedstock. This model is based on the fact that the powder can be regarded as rigid. Thus the deformation in a shear field has to be taken by the binder (**Figure 11**, right), which means that the binder is sheared more, resulting in a lower viscosity of the binder (due to the shear thinning behavior of a polymer [43]). All together the viscosity is shifted to higher values by higher powder loading and somewhat decreased by higher dissipation inside the polymer due to enhanced shear strain (**Figure 11**, red arrow).

## 2.5. Temperature influence

One generally neglected effect on the measured viscosity data is the rise of the temperature due to dissipation. In a standard measurement setup of a high-pressure capillary rheometer, a temperature is chosen and set in the control unit. Usually there is no temperature transducer mounted inside the flow channel. Thus, the set temperature value is assigned to the derived viscosity curve.

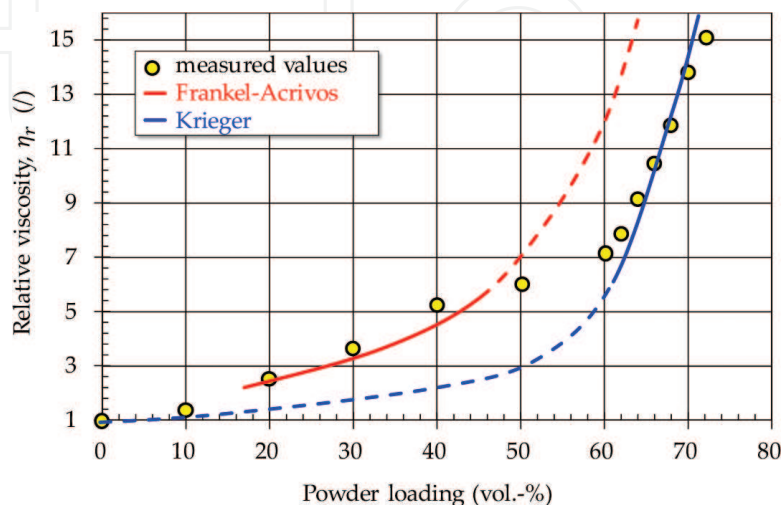


**Figure 10.** Comparison of measured with predicted values of relative viscosity  $\eta_r$ , [41].



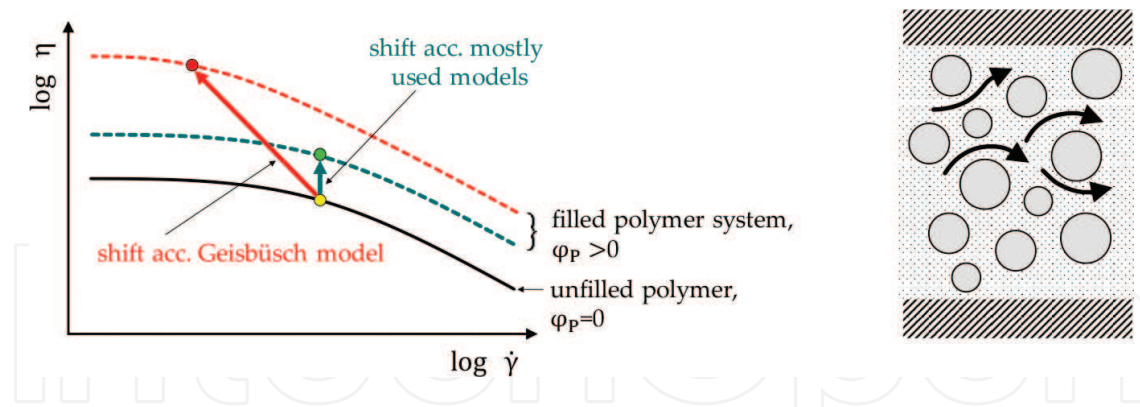


**Figure 11.** Schematic viscosity diagram of a filled polymer system; shift acc. Geisbüsch and mostly used model (left), shear enhancement in the binder (right).

But in reality, a certain heat dissipation takes place. The assumption of isothermal conditions is only applicable if the related rise in temperature is small. For unfilled polymers, this effect cannot be neglected at very high shear rates only ( $10^5$  to  $10^6$   $s^{-1}$ ). In our case of stiff fillers (between 50 and 60 vol% of filler), nearly all the dissipated heat is generated in the matrix, since the stiff filler is more or less just 'swimming' with the flow of the polymer (**Figure 11** right). As reported previously [44], at a shear rate above  $100$   $s^{-1}$ , nearly all dissipated heat will stay in the polymer resulting in a higher temperature and at the same time a lower viscosity of the polymer. Therefore, the actual temperature, which should be assigned to a specific value of viscosity, is higher than the normally used one. Using the actual temperature data gives in the end a flatter viscosity curve.

#### 2.5.1. Temperature development in the slit die and temperature correction

Rheological measurements on unfilled polymers [45–47] and on MIM feedstocks [33, 35, 44] show an initial increase of the measured die wall temperature.

**Figure 12** shows, as an example, the measured temperature profiles of the die wall temperatures for 316 L MIM feedstock from experimental measurements with the slit die on HPCR at  $190^\circ C$ .

The analysis clearly shows (**Figure 12**) the increase of the temperature due to shear dissipation from an apparent shear rate up to approximately 7 K at the highest shear rate of  $10^3$   $s^{-1}$ . Thus, the measured data needs to be corrected with respect to temperature. So the melt temperature rise due to dissipative heating and compression heat was taken into account by applying a special temperature correction procedure [45]. For this purpose, a thermodynamic dimensionless number, the so-called Cameron number [48], is used, and the temperature corrected viscosity is obtained. Utilizing a modified Agassant method [45, 49], the average melt temperature inside the flow channel is calculated and applied to adjust the viscosity. The shear viscosities obtained under varying temperatures can be transformed into a single master curve by applying the time-temperature superposition principle [45, 49].

Estimation of temperature rise in a polymer highly filled with stiff powders and the related viscosity correction.

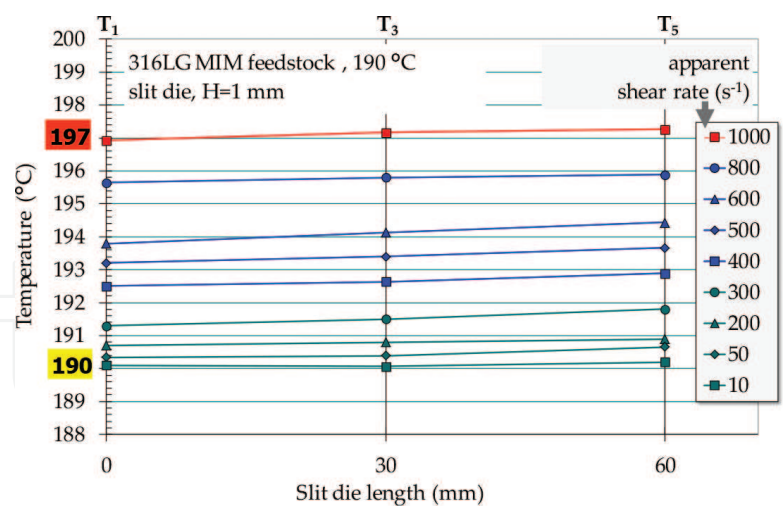


Figure 12. Temperature profiles at different shear rates (slit die) [35].

In injection molding of highly filled polymers, high shear rates occur. Since the fillers are stiff, all the shear has to be taken up by the polymer system. In case of high shear rates, one has to consider whether due to the short times the generated heat stays to a high extent in the polymer or it is conducted into the powder. Therefore, we evaluated the contribution of viscous dissipation over the heat conduction normal to the direction of flow by calculating the Griffith number ( $Gr$ ). The calculation of  $Gr$  showed that at high shear rates (higher than  $100\text{ s}^{-1}$ ), the heat generated in the binder due to viscous dissipation is larger than the heat transmitted by conduction to the metal particles (i.e.,  $Gr > 1$ ), and thus, the binder will have higher temperature than the filler particles [44].

Using the estimated temperature rise, one can correct the viscosity at high shear rates and use the model proposed by Geisbüsch [42] to predict the measured data. This is shown in **Figure 13** for the particular example of 60 vol% MIM feedstock. The viscosity values were shifted by using the Arrhenius equation, and it can be seen that the prediction from the model has improved at the higher shear rates [44].

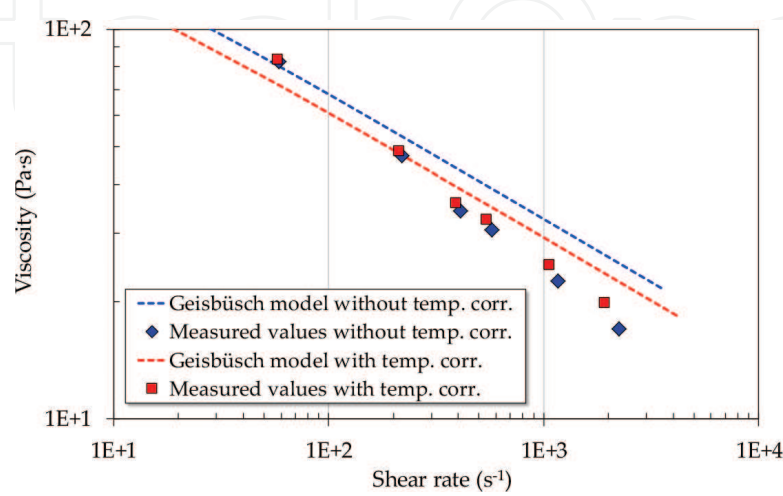
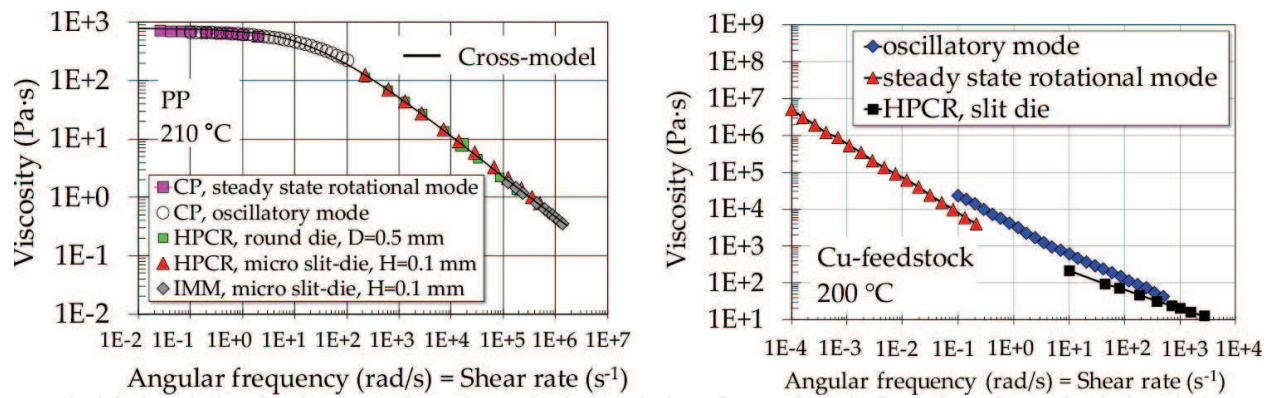


Figure 13. Viscosity corrections due to temperature increase at high shear rates and predictions by the Geisbüsch model for 60 vol% feedstock [44].



**Figure 14.** Cox-Merz rule as an example for unfilled polypropylene [49, 50] (left) and for highly filled Cu feedstock (right); CP—Cone-plate rheometer, HPCR—High-pressure capillary rheometer, and IMM—Injection molding rheometer.

## 2.6. Cox-Merz rule and highly filled polymers

The rheological behavior of highly filled polymers is a complex function of its physical properties and the processes that occur at the scale of the suspended particles. Therefore, there are special considerations that do not apply to highly filled polymers but are applicable to unfilled polymers. For example, the Cox-Merz rule [17], which states that the viscosity measured in oscillatory mode is equivalent to the viscosity measured in steady-state rotational mode or in a capillary rheometer (**Figure 14**, left). The Cox-Merz rule is quite useful to extend the range of shear rates or angular frequencies, where the viscosity can be measured without sample fracture, secondary flows, and material expulsion. However, for highly filled systems, it does not apply as shown in **Figure 14**, right. In oscillatory mode, the viscosity values (complex viscosity) tend to be overestimated with respect to the measurements obtained in steady-state rotational mode or by high-pressure capillary rheometry.

## 3. Viscosity models

The mathematical model describing quantitatively the relation between shear stress and the shear strain during flow of the polymeric fluids is called the constitutive equation. Even though the molecular structure and viscoelasticity of polymeric materials are quite complicated, various forms of constitutive equations have been proposed.

In order to describe, for example, the injection molding process, a viscosity function is necessary, which is valid over the whole process range. The viscosity as a function of temperature, shear rate, and pressure is needed for the calculation of the filling and holding pressure phase; it has an effect on the pressure calculation and the holding pressure efficiency.

For the injection molding simulation, it is very important to describe the viscosity, as the shear rate approaches zero, as accurately as possible. This behavior is significant in the post-pressure phase because here the melt speeds are very small overall. In addition, even during the faster filling phase, due to a symmetrical velocity profile, the shear rate in the middle of the channel is zero. For highly filled polymers at low shear rates ( $<0.1 \text{ s}^{-1}$ ), the viscosity increases and a yield point can occur (**Figure 15**). This means that viscous flow is only observed above a

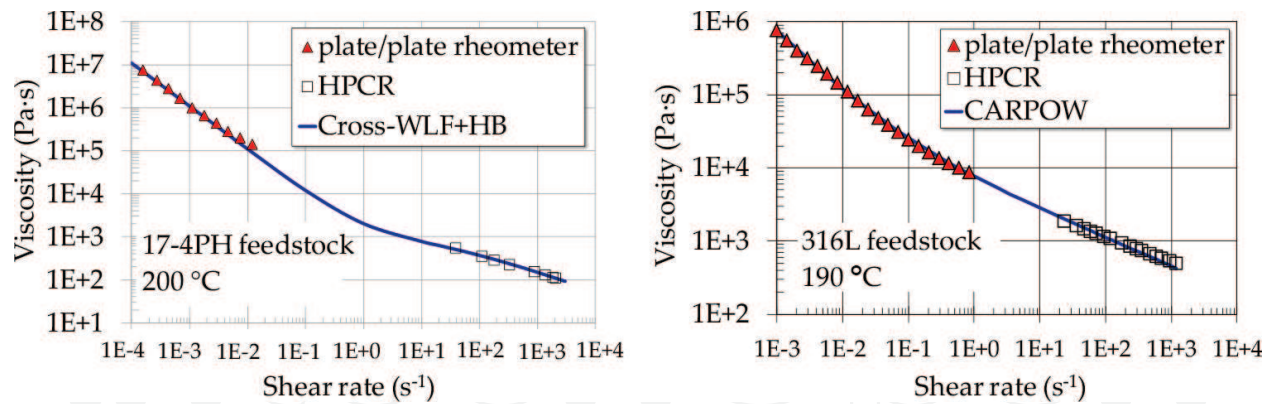


**Figure 15.** Approximation of the viscosity curve of two different feedstocks using Cross-WLF model with Herschel-Bulkley (HB) extension (left) and CARPOW model (right).

Model	Equation of the model	
Cross-WLF with Herschel-Bulkley extension	$\eta = \frac{\eta_0}{1 + \left(\frac{\eta_0 \cdot \dot{\gamma}}{D_4}\right)^{(1-n)}} + \tau_\gamma \cdot \left(\frac{1 - e^{(-\alpha \dot{\gamma})}}{\dot{\gamma}}\right) \quad [51]$	(10)
	$\eta = \frac{\eta_0}{1 + \left(\frac{\eta_0 \cdot \dot{\gamma}}{D_4}\right)^{(1-n)}} + \frac{\tau_{y0} \cdot e^{\left(\frac{T}{T_y}\right)}}{\dot{\gamma}} \quad [52]$	(11)
	$\eta_0 = D_1 \cdot e^{\left[\frac{-A_1(T-T_0)}{A_2(T+T_0)}\right]}, \quad T_s = D_2 + D_3 \cdot p, \quad A_2 = \tilde{A}_2 + D_3 \cdot p$	
CARPOW	$\eta = \frac{d_c \cdot a_T}{(a_i \cdot b_i + \dot{\gamma})^{n_i}} + \frac{A \cdot a_T}{(1 + \dot{\gamma} \cdot B \cdot a_T)^C} \quad [53]$	(12)

where  $D_1, D_2, D_3, D_4$ —cross coefficients,  $\eta_0$ —zero shear viscosity,  $\tau_\gamma, \alpha$  and  $\tau_{y0}, T_y$ —coefficients of Herschel-Bulkley extension,  $\dot{\gamma}$ —shear rate,  $A_1, A_2, \tilde{A}_2$ —Williams-Landel-Ferry (WLF) coefficients,  $p$ —pressure,  $T$ —temperature,  $T_s$ —reference temperature,  $a_T$ —temperature shift factor acc. Arrhenius or WLF,  $d_c$ —consistency parameter (toughness of the highly filled system),  $b_i$ —turning point of the viscosity curve,  $n_i$ —flow exponent of low shear rate range, and  $A, B, C$ —Carreau coefficients.

**Table 1.** Selected models to describe shear rate and temperature dependents of viscosity.

minimum wall shear stress. As mentioned before, the cause of this phenomenon is an interaction of the filler particles with each other or with the polymer matrix. Due to the increase in viscosity at low shear rates, the behavior of highly filled polymers in the low shear rate range resembles that of a solid rather than a polymer melt.

For the description of the temperature-dependent flow behavior in a wide shear rate range of unfilled and little-filled polymers, a number of viscosity models have been published, such as the well-known Carreau model and Cross model [43, 48]. The flow behavior of highly filled polymer compounds like MIM feedstocks can be described with the models shown in **Table 1**. These viscosity models offer the opportunity to approximate the measured viscosity data at low shear rates with yield stress and the viscosity at high shear rates with shear thinning behavior. Examples of the fit of these models are given in **Figure 15**.



## 4. Conclusion

Good rheological data are necessary for a proper optimization of the production using highly filled polymers and also for good simulations of the related production processes. Since simulation of a production process needs a good virtual model of this process, the correct understanding of the occurring physical effects is vital.

Rheology of highly filled polymers is the tool in place to gain such a deeper understanding. On the other hand, it is essential to have this understanding when measuring reliable rheological data of such materials, which show special and characteristic behavior like yield stress or dependency on the powder loading and shear rate.

## Acknowledgements

The researchers acknowledge the Polymer Competence Center Leoben (PCCL) for providing the rotational rheometer for measurements.

## Author details

Christian Kukla<sup>1\*</sup>, Ivica Duretek<sup>2,3</sup>, Joamin Gonzalez-Gutierrez<sup>2</sup> and Clemens Holzer<sup>2</sup>

\*Address all correspondence to: [christian.kukla@unileoben.ac.at](mailto:christian.kukla@unileoben.ac.at)

1 Industrial Liaison Department, Montanuniversitaet Leoben, Leoben, Austria

2 Department of Polymer Engineering and Science, Montanuniversitaet Leoben, Leoben, Austria

3 Polymer Competence Center Leoben GmbH, Leoben, Austria

## References

- [1] Rueda MM, Auscher M-C, Fulchiron R, Périé T, Martin G, Sonntag P, Cassagnau P. Rheology and applications of highly filled polymers: A review of current understanding. *Progress in Polymer Science*. 2017;**66**:22-53. DOI: 10.1016/j.progpolymsci.2016.12.007
- [2] Mewis J, Wagner NJ. *Colloidal Suspension Rheology*. Cambridge, UK: Cambridge University Press; 2011. 393 pp
- [3] Eilers H. Die Viskosität von Emulsionen hochviskoser Stoffe als Funktion der Konzentration. *Kolloid-Zeitschrift*. 1941;**97**:313-321. DOI: 10.1007/BF01503023



- [4] Einstein A. Eine neue Bestimmung der Moleküldimensionen [Dissertation]. Zürich: Universität Zürich; 1906
- [5] Einstein A. Berichtigung zu meiner Arbeit. *Annals of Physics*. 1911;591-592. DOI: 10.1002/andp.19113390313
- [6] Frankel NA, Acrivos A. On the viscosities of a concentrated suspension of solid spheres. *Chemical Engineering Science*. 1967;22:847-853. DOI: 10.1016/0009-2509(67)80149-0
- [7] Janardhana Reddy J, Ravi N, Vijayakumar M. A simple model for viscosity of powder injection moulding mixes with binder content above powder critical binder volume concentration. *Journal of the European Ceramic Society*. 2000;20:2183-2190. DOI: 10.1016/S0955-2219(00)00096-0
- [8] Kate KH, Enneti RK, Park SJ, German RM, Atre SV. Predicting powder-polymer mixture properties for PIM design. *Critical Reviews in Solid State and Materials Sciences*. 2014;39:197-214. DOI: 10.1080/10408436.2013.808986
- [9] Krieger IM, Dougherty TJ. A mechanism for non-Newtonian flow in suspensions of rigid spheres. *Transactions of the Society of Rheology*. 1959;3:137-152. DOI: 10.1122/1.548848
- [10] Mooney M. The viscosity of a concentrated suspension of spherical particles. *Journal of Colloid Science*. 1951;6:162-170. DOI: 10.1016/0095-8522(51)90036-0
- [11] Mueller S, Llewellyn EW, Mader HM. The rheology of suspensions of solid particles. *Proceedings of the Royal Society A: Mathematical, Physical and Engineering Sciences*. 2010;466:1201-1228. DOI: 10.1098/rspa.2009.0445
- [12] Gonzalez-Gutierrez J, Duretek I, Kukla C, Poljšak A, Bek M, Emri I, Holzer C. Models to predict the viscosity of metal injection molding feedstock materials as function of their formulation. *Metals*. 2016;6:129. DOI: 10.3390/met6060129
- [13] Pabst W. Fundamental considerations on suspension rheology. *Ceramics – Silikáty*. 2004;48(1):6-13
- [14] Gonzalez-Gutierrez J, Godec D, Guran R, Spoerk M, Kukla C, Holzer C. 3D printing conditions determination for feedstock used in fused filament fabrication (FFF) of 17-4PH stainless steel parts. *Metallurgia*. 2018;57:117-120
- [15] Gonzalez-Gutierrez J, Stringari GB, Emri I. Powder injection molding of metal and ceramic parts. In: Wang J, editor. *Some Critical Issues for Injection Molding*. Rijeka, Croatia: InTech; 2012. pp. 65-86. DOI: 10.5772/38070
- [16] Kukla C, Duretek I, Gonzalez-Gutierrez J, Holzer C. Rheology of PIM feedstocks. *Metal Powder Report*. 2017;72:39-44. DOI: 10.1016/j.mprp.2016.03.003
- [17] Cox WP, Merz EH. Correlation of dynamic and steady flow viscosities. *Journal of Polymer Science*. 1958;28:619-622. DOI: 10.1002/pol.1958.1202811812
- [18] Stickel JJ, Powell RL. Fluid mechanics and rheology of dense suspensions. *Annual Review of Fluid Mechanics*. 2005;37:129-149. DOI: 10.1146/annurev.fluid.36.050802.122132

- [19] Pahl M, Gleißle W, Laun H-M. *Praktische Rheologie der Kunststoffe und Elastomere*. Dusseldorf, Germany: VDI-Verlag; 1991. 454 pp
- [20] Bagley EB. End corrections in the capillary flow of polyethylene. *Journal of Applied Physics*. 1957;**28**:624-627. DOI: 10.1063/1.1722814
- [21] Eisenschitz R, Rabinowitsch B, Weissenberg K. Zur Analyse des Formveraenderungswiderstandes. *Mitteilungen der deutschen Materialspruefungsanstalten*. 1929;**9**:91-94. DOI: 10.1007/978-3-642-92045-5\_11
- [22] Wales JLS, den Otter JL, Janeschitz-Kriegl H. Comparison between slit viscometry and cylindrical capillary viscometry. *Rheologica Acta*. 1965;**4**:146-152. DOI: 10.1007/BF01984712
- [23] Tadmor Z, Klein I. *Engineering Principles of Plasticating Extrusion*. New York: Van Nostrand Reinhold; 1970. 500 pp
- [24] Eswaran R, Janeschitz-Kriegl H, Schijf J. A slit viscometer for polymer melts. *Rheologica Acta*. 1963;**3**:83-91. DOI: 10.1007/BF01979457
- [25] Laun HM. Polymer melt rheology with a slit die. *Rheologica Acta*. 1983;**22**:171-185. DOI: 10.1007/BF01332370
- [26] Nyborg L, Johansson E, Niederhauser S. Assessment of rheology and related properties of PIM feedstock material. In: *Euro PM200 Proceedings. 2nd European Symposium on Powder Injection Moulding*; 18-20 October, Munich. Shrewsbury, UK: EPMA; 2000. pp. 67-74
- [27] Bilovol VV. *Mould filling simulations during powder injection moulding [PhD thesis]*. Delft, The Netherlands: Delft University of Technology; 2003
- [28] Friesenbichler W, Duretek I. Rheologische Charakterisierung hochgefüllter PIM-Feedstocks und Holzcompounds. In: *Tagungshandbuch zum 17. Leobener Kunststoffkolloquium. 17. Leobener Kunststoffkolloquium*; 20-21 November, Leoben, Austria. Leoben, Austria: Montanuniversitaet Leoben; 2003. pp. XIX-1-XIX-24
- [29] Han CD. On intrinsic errors in pressure-hole measurements in flow of polymer melts. *AIChE Journal*. 1972;**18**:116-121. DOI: 10.1002/aic.690180121
- [30] Walters K. *Rheometry*. New York: John Wiley & Sons Inc; 1975. 278 pp
- [31] Chastagner MW. *Slit die rheology of HDPE and ABS based wood plastic composites [master thesis]*. Pullman, WA, USA: Washington State University; 2005
- [32] Feldbacher G. *Rheologische und thermodynamische Stoffdatenerfassung von zwei Thermoplasten für die FEM Werkzeugauslegung [bachelor thesis]*. Leoben, Austria: Montanuniversitaet Leoben; 2003
- [33] Atakan Y. *Ermittlung der Fließfähigkeit und Plastifizierarbeit von handelsüblichen MIM-Feedstocks [master thesis]*. Leoben, Austria: Montanuniversitaet Leoben; 2008

- [34] MATLAW Consortium. Final Report MATLAW: New material laws for metal filled injection moulding feedstocks [Internet]. 15.01.2009. Available from: [http://cordis.europa.eu/publication/rcn/11893\\_en.html](http://cordis.europa.eu/publication/rcn/11893_en.html) [Accessed 2018-01-23]
- [35] Duretek I. Untersuchungen zum Fließverhalten von Metall-, Keramik- und Holz-Kunststoffverbunden [PhD thesis]. Leoben, Austria: Montanuniversitaet Leoben; 2013
- [36] Liddell PV, Boger DV. Yield stress measurements with the vane. *Journal of Non-Newtonian Fluid Mechanics*. 1996;**63**:235-261. DOI: 10.1016/0377-0257(95)01421-7
- [37] Sun A, Gunasekaran S. Yield stress in foods: Measurements and applications. *International Journal of Food Properties*. 2009;**12**:70-101. DOI: 10.1080/10942910802308502
- [38] Dapčević T, Dokić P, Hadnađev M, Pojić M. Determining the yield stress of food products: Importance and shortcomings. *Food Processing, Quality and Safety*. 2008;**35**:143-149
- [39] Duretek I, Kukla C, Langecker GR, Holzer C. Measurement of the yield stress of a stainless steel feedstock. In: *Euro PM2013 Proceedings. Euro PM2013 Congress & Exhibition; 15-18 September, Gothenburg, Sweden*. Bellstone: EPMA; 2013
- [40] Kukla C, Duretek I, Holzer C. Controlled shear stress method to measure yield stress of highly filled polymer melts. *AIP Conference Proceedings*. 2016;**1779**:070006-1 to 070006-5. DOI: 10.1063/1.4965538
- [41] Kukla C, Duretek I, Holzer C. Modelling of rheological behaviour of 316L feedstocks with different powder loadings and binder compositions. In: *Euro PM2014 Proceedings. Euro PM2014 Congress and Exhibition; 21-24.09; Salzburg, Austria*. Bellstone: EPMA; 2014. pp. 1-6
- [42] Geisbüsch P. Ansätze zur Schwindungsberechnung ungefüllter und mineralisch gefüllter Thermoplaste [PhD thesis]. Aachen: RWTH Aachen; 1980
- [43] Osswald TA, Hernandez-Ortiz JP. *Polymer Processing: Modeling and Simulation*. Munich: Carlo Hanser Verlag; 2006. 597 pp
- [44] Kukla C, Duretek I, Schuschnigg S, Gonzalez-Gutierrez J, Gooneie A, Holzer C. Study of rheological behaviour of stainless steel feedstock taking into account the thermal effects. In: *Rasteiro MG, editor. Ibero 15: Conference Proceedings; Coimbra, Portugal: University of Coimbra*. 2015. pp. 46-49
- [45] Friesenbichler W, Langecker GR, Duretek I, Schuschnigg S. Polymer melt rheology at high shear rates using a new micro-rheology technique. In: *Proceedings of 21st Annual Meeting of the Polymer Processing Society*. 6.1-1-6.1-15
- [46] Duretek I, Friesenbichler W, Schuschnigg S, Rajganes J, Langecker GR. Study on rheological behaviour of polymer melts at high shear rates using a new micro-rheology technique. In: *Proceedings of Past and Future of Polymer Processing, Technology and Science; 27-28 April; Zagreb, Croatia*. 2006
- [47] Friesenbichler W, Duretek I, Rajganes J, Selvasankar RK. Measuring the pressure dependent viscosity at high shear rates using a new rheological injection mould. *Polimery*. 2011;**56**(1):58-62

- [48] Agassant JP, Sergent P, Avenas JF, Carreau PJ. Polymer Processing: Principles and Modelling. Cincinnati, OH, USA: Hanser Gardner; 1991. 846 pp
- [49] Schuschnigg S. Rheologische Untersuchungen bei hohen Schergeschwindigkeiten mit Hilfe eines Mikrorheologie-Schlitzdüsen Messsystems [master thesis]. Leoben, Austria: Montanuniversitaet Leoben; 2004
- [50] Cramer A, Michaeli W, Friesenbichler W, Duretek I. Simulation des Spritzgießprozesses von Mikrobautteilen. Zeitschrift Kunststofftechnik Journal of Plastics Technology. 2007;1-26
- [51] SIGMA Engineering. SIGMASOFT 5.0+: Manual. SIGMA Engineering GmbH: Aachen, Germany; 2013
- [52] CoreTech System. Moldex3D R15.0: Manual. New Taipei City, Taiwan: CoreTech System Co., Ltd; 2017
- [53] Erb T, Geiger K, Bonten C. Mixing processes—Influence of the viscosity model on flow calculations. AIP Conference Proceedings. 2014;**1593**:549-555. DOI: 10.1063/1.4873841

IntechOpen

